Severe Occlusive Carotid Artery Disease: Hemodynamic Assessment by MR Perfusion Imaging in Symptomatic Patients

Masayuki Maeda, William T. C. Yuh, Toshihiro Ueda, Joan E. Maley, Daniel L. Crosby, Ming-Wang Zhu and Vincent A. Magnotta

AJNR Am J Neuroradiol 1999, 20 (1) 43-51
http://www.ajnr.org/content/20/1/43

AJNR Am J Neuroradiol 20:43–51, January 1999

Severe Occlusive Carotid Artery Disease: Hemodynamic Assessment by MR Perfusion Imaging in Symptomatic Patients

Masayuki Maeda, William T. C. Yuh, Toshihiro Ueda, Joan E. Maley, Daniel L. Crosby, Ming-Wang Zhu, and Vincent A. Magnotta

BACKGROUND AND PURPOSE: **Cerebral hemodynamic status has been reported to influence the occurrence and outcome of acute stroke. The purpose of this study was to assess hemodynamic compromise in symptomatic patients with severe occlusive disease of the carotid artery by the use of echo-planar perfusion imaging.**

METHODS: **Spin-echo echo-planar perfusion imaging was performed in 11 patients (two had bilateral disease) with severe stenosis or occlusion of the carotid artery who had experienced either a recent transient ischemic attack or minor stroke. Relative cerebral blood volume (rCBV) maps and relative mean transit time (rMTT) maps were generated from the time-concentration curve. Findings on T2-weighted images, angiograms, rCBV maps, and rMTT maps were compared and assessed qualitatively and quantitatively.**

RESULTS: **Although the abnormalities on T2-weighted images were absent, minimal, and/or unrelated to the degree of stenosis or collateral circulation, rMTT maps showed much larger and more distinct perfusion abnormalities along the vascular distribution of the affected vessels in all 13 vascular territories of the 11 patients. Despite obvious abnormalities on rMTT maps, none of the patients had evidence of decreased rCBV in the affected brain tissue (increased in three, normal in eight). A statistically significant difference in rMTT values was found between the affected and unaffected brain tissue, whereas no significant difference was seen in rCBV values.**

CONCLUSION: **Echo-planar perfusion imaging is a noninvasive and rapid method for evaluating the hemodynamics in severe occlusive carotid artery disease and the compensatory vascular changes, and it may be useful in patient management.**

The cerebral hemodynamic status of patients with severe occlusive carotid artery disease has been reported to play a significant role in the occurrence of stroke (1). Two mechanisms of cerebral ischemia in this disease have been identified: vascular occlusion from an embolism or propagating thrombus from an atherosclerotic plaque of the carotid artery (artery-to-artery embolism), and watershed or border-zone ischemia caused by critically reduced perfusion pressure (hemodynamic stroke). Insufficient collateral circulation may cause a critical reduction in cerebral blood flow (CBF) and an increased risk of hemodynamic stroke. It is well known that hypoperfused tissue under chronic hemodynamic stress may undergo compensatory changes, which can be difficult to diagnose with conventional CT or MR imaging (2) in patients who are also at increased risk for a major stroke (3). Therefore, a noninvasive and convenient means to detect and evaluate the underlying hemodynamic compromise in symptomatic patients with severe stenosis or occlusion of the carotid artery may be helpful in the diagnosis and management of this common disease.

Technological advances have made it possible to obtain direct and more accurate measurements of the regional hemodynamics of brain tissue, such as regional CBF and regional cerebral blood volume (CBV) by using positron emission tomography (PET); however, this type of hemodynamic information has not been widely applied in the clinical setting, because the availability of PET is limited by its cost and technical complexity. In addition, PET cannot provide prompt information, making it impractical in the management of acute stroke. Recently, the development of perfusion MR imaging has made the rapid assessment of cerebral hemodynamics possible (4–10). Although this method,

Received November 7, 1997; accepted after revision August 31, 1998.

From the Department of Radiology, The University of Iowa College of Medicine, 200 Hawkins Dr, Iowa City, IA 52242.

Address reprint requests to William T. C. Yuh, MD.

TABLE 1: Data for 11 patients with chronic cerebral ischemia

Patient	Age (y)/Sex	Symptoms	Angiographic Findings (%)	Findings on T2-Weighted Images	Prolonged MTT on MTT Maps	CBV Asymmetry on CBV Maps
1	41/F	L hemiparesis	R ICA stenosis (50)	R watershed infarction	R MCA	Decreased CBV in R watershed infarction
2	62/F	TIA	R ICA stenosis (95)	Normal	R MCA	None
3	62/F	TIA	R ICA stenosis (80)	Normal	R MCA	None
4	74/F	TIA	R ICA stenosis (90)	Bil multiple lacunar infarctions	R MCA	None
5	84/F	TIA	R ICA stenosis (99)	R watershed infarction	R MCA and ACA	Increased CBV in R ACA and MCA Decreased CBV in R watershed infarction
6	73/F	L hemiparesis	R ICA occlusion	R watershed infarction	R MCA and ACA	Increased CBV in R ACA and MCA Decreased CBV in R watershed infarction
7	73/F	None	R ICA occlusion	R basal ganglia infarction	R MCA	None
8	60/F	L hemiparesis	R ICA occlusion	Bil multiple lacunar infarctions	R MCA	Increased CBV in R MCA
9	46/M	TIA	R ACA occlusion	Bil multiple lacunar infarctions	R ACA	None
10	44/M	TIA	Bil ICA occlusions	Bil multiple lacunar infarctions R watershed infarction	Bil MCA and ACA	Decreased CBV in R watershed infarction
11	55/F	TIA	Bil ICA occlusions	R lacunar infarction	Bil MCA and ACA	None

Note.—TIA indicates transient ischemic attack; ICA, internal carotid artery; ACA, anterior cerebral artery; MCA, middle cerebral artery; Bil, bilateral; MTT, mean transit time; CBV, cerebral blood volume.

unlike PET, cannot provide absolute measurements of CBV or CBF, it can offer a semiquantitative assessment of relative CBV (rCBV) and vascular mean transit time (rMTT) more promptly than with PET. By using echo-planar perfusion imaging (EPPI) techniques, multisection images can be readily obtained to cover the symptomatic brain within a very short time frame (8–10), which is essential for feasibility within the clinical setting.

Our purpose was to assess the usefulness of EPPI in the detection and evaluation of the underlying hemodynamic compromise in patients with severe stenosis or occlusion of the carotid artery who had experienced either a recent transient ischemic attack (TIA) or minor stroke.

Methods

Patients

Eleven patients (two men and nine women) aged 41 to 84 years (mean age, 61 years) with severe stenosis or occlusion of the carotid artery who had experienced either a recent TIA or minor stroke were studied. All patients underwent angiography, which demonstrated unilateral occlusion of the internal carotid artery (ICA) (n = 3), unilateral stenosis of the ICA (n = 5), bilateral occlusion of the ICA (n = 2), or unilateral occlusion of the anterior cerebral artery (ACA) (n = 1). Cerebral angiography was performed within 8 hours of the perfusion MR study. Patients' symptoms, usually TIA or minor stroke, are summarized in Table 1.

MR Studies

MR studies were performed on a 1.5-T MR unit retrofitted for echo-planar imaging (EPI) capabilities. Axial T1- and T2-weighted standard spin-echo sequences were obtained before EPPI with imaging parameters of 600/20/1,2 (TR/TE/excitations) for T1-weighted images and 2000–2500/30,90/1,2 for T2-weighted double-echo images, with a section thickness of 5 mm, a matrix of 256 × 192, and a field of view of 24 cm. Dynamic spin-echo EPI susceptibility-contrast images were obtained with 8 to 10 axial sections at 2-second intervals for 60 seconds with imaging parameters of 2000/100/1, a field of view of 20 × 40, a 128 × 256 acquisition matrix, single shot. Approximately four to five images per section were obtained before the start of an IV bolus injection (9 mL/s) of 0.1 mmol/kg of gadopentetate dimeglumine using an MR-compatible power injector.

The theory of nondiffusable tracers was applied to these data. Since no arterial input function was available, only relative regional measurements were obtained. Although rMTT calculations cannot be performed without a complete understanding of the topology of the vasculature (11), important information about tissue perfusion is provided by rMTT calculations, especially when corresponding hemispheres are compared. Because of susceptibility effects, signal intensity drops as the contrast material reaches the tissue and corresponds to relative tissue perfusion. A plot relaxivity (δR_2^*) or $1/T_2^*$ versus time is the first step in quantitative analysis and is assumed to be directly proportional to the concentration-time curve.

$$\Delta R_2^* = \left[-\ln\left(\frac{SI(t)}{SI_0}\right) \Big/ TE \right] \quad (1)$$

where $SI(t)$ is the signal intensity at time t, and SI_0 is the signal intensity before the arrival of contrast material. SI_0 was calculated as the average signal intensity over the first four images.

A least-squares optimization to fit a four-parameter γ variate model of the δR_2^* versus time curve (equation 2) (11) was then determined.

2) $$R_2^*(t) = \kappa(t - t_a)^{\alpha} e^{[-(t-t_a)]/\beta}$$

This facilitated the determination of starting and ending times for the first pass of contrast material, thus eliminating second and additional passes of contrast material from showing up in the computation of rCBV and rMTT values. rCBV was defined as the area under the δR_2^* curve. rMTT was calculated as the ratio of the first moment of the δR_2^* curve and rCBV (9, 12–14).

3) $$rCBV = \int_{t_a}^{t_e} \Delta R_2^* \, dt$$

and

4) $$rMTT = \frac{\int_{t_a}^{t_e} t\Delta R_2^* \, dt}{\int_{t_a}^{t_e} \Delta R_2^* \, dt}$$

where t_a was the starting time and t_e was the ending time of the first pass of contrast material as found from the least-squares fit of the γ variate model of the δR_2^* curve. rMTT and rCBV maps of the brain were generated by computing an rMTT and rCBV at each pixel in the image. Numerical integration of the base line–corrected δR_2^* curve was performed using Simpson's rule. To avoid excess noise in the calculations, rCBV and rMTT values were computed using a 5×5 mask. To reduce the time required to generate the maps, the brain parenchyma was segmented from the image automatically by first applying a threshold to the image, which provided a means to segment the brain, scalp, and eyes from the background. A 3×3 square was then used as a structuring element for image erosion. The eroded image was dilated with a 5×5 square structuring element. This provided a reliable automatic means of segmenting the brain parenchyma and also of markedly improved the computation time.

Our in-house software numerically generated the rCBV and rMTT maps from the first-pass portion of the δR_2^* versus time curve. This was completed automatically in less than 4 minutes for 11 sections on a SUN SPARC2 workstation. The maps were scaled and saved in an image format that could be transferred to the scanner and filmed for the radiologist to review. Total time for the acquisition and processing of the EPPI was approximately 10 minutes.

Normal rCBV maps showed higher signal intensity in gray matter than in white matter, indicating greater rCBV in gray matter, whereas normal rMTT maps showed lower signal intensity (secondary to T2* effect) in gray matter than in white matter, suggesting more blood supply to the gray matter. Ischemic tissue with prolonged rMTT showed higher signal intensity than that of normal tissue. Normal rCBV and rMTT maps showed symmetric signal intensity in both the gray and white matter of the two hemispheres and in the anterior and posterior circulation.

Data Analysis

Angiograms were reviewed for evidence of chronic occlusion or degree of stenosis of the proximal vessels and collateral circulation inside or outside (mainly the external carotid artery [ECA] to the ICA) the circle of Willis. Conventional MR studies were reviewed for evidence of signal abnormality on T2-weighted images.

rCBV and rMTT maps were qualitatively assessed by three neuroradiologists in a side-by-side comparison with the corresponding T2-weighted images obtained at similar section levels. Qualitative analysis of these perfusion maps was based on visual assessment of the relative difference in signal intensity between both hemispheres and the anterior and posterior circulation on both the rMTT and rCBV maps. The final decision was reached by consensus. Angiographic findings were shown to observers after assessment of the T2-weighted images and the rMTT and rCBV maps.

In the quantitative analysis, region-of-interest (ROI) measurements of signal intensity were performed where the rMTT maps showed high signal intensity in nine patients with unilateral artery occlusion or stenosis. ROIs were chosen by tracing the brain tissue with prolonged rMTT. The rCBV maps were also measured using the same ROI territory chosen in the rMTT map. Corresponding T2-weighted images were reviewed, and care was taken to avoid placing the ROI over old infarcted areas. Contralateral ROIs were also chosen from anatomically symmetric sites for comparison. In each case, quantitative analysis and selection of ROIs were performed in several different contiguous images, because abnormal rMTT maps were usually seen not only in a single axial section but also extended in the craniocaudal direction in the territory of the affected vessel. The mean value of the rMTT and rCBV was obtained from the quantitative analysis of all the contiguous images with abnormal rMTT.

Statistical Analysis

A paired *t*-test (two-tailed) was used to evaluate the significant difference in mean rCBV and rMTT values between the affected and contralateral sides. Differences between the means were considered significant if the *P* values were below the .05 level of confidence ($P < .05$).

Results

Angiographic Findings

Angiographic findings are summarized in Table 1. In four patients with unilateral stenosis of the ICA (patients 1 through 4), the blood supply of the middle cerebral artery (MCA) on the affected side was mainly antegrade via the ipsilateral ICA. In four patients with unilateral occlusion or preocclusive stenosis of the ICA (patients 5 through 8), the MCA supply on the affected side was via the ipsilateral ophthalmic artery from the ipsilateral ECA in two patients (patients 5 and 6), via anastomotic channels across the surface of the brain from the ipsilateral ACA in one patient (patient 8), and via the anterior circle of Willis from the opposite carotid circulation in one patient (patient 7). In one patient with unilateral occlusion of the ACA (patient 9), the ACA on the affected side received pial collaterals from the ipsilateral MCA. In two patients with bilateral ICA occlusion (patients 10 and 11), bilateral MCAs and ACAs were via the posterior circle of Willis from the vertebral arteries.

Findings on T2-Weighted Images

T2-weighted images showed either no (n = 2) or minimal (n = 9) abnormality, revealing small lacunar or watershed infarctions (Table 1). Abnormal T2-weighted changes were noted on the ipsilateral (six patients) or contralateral (three patients) side.

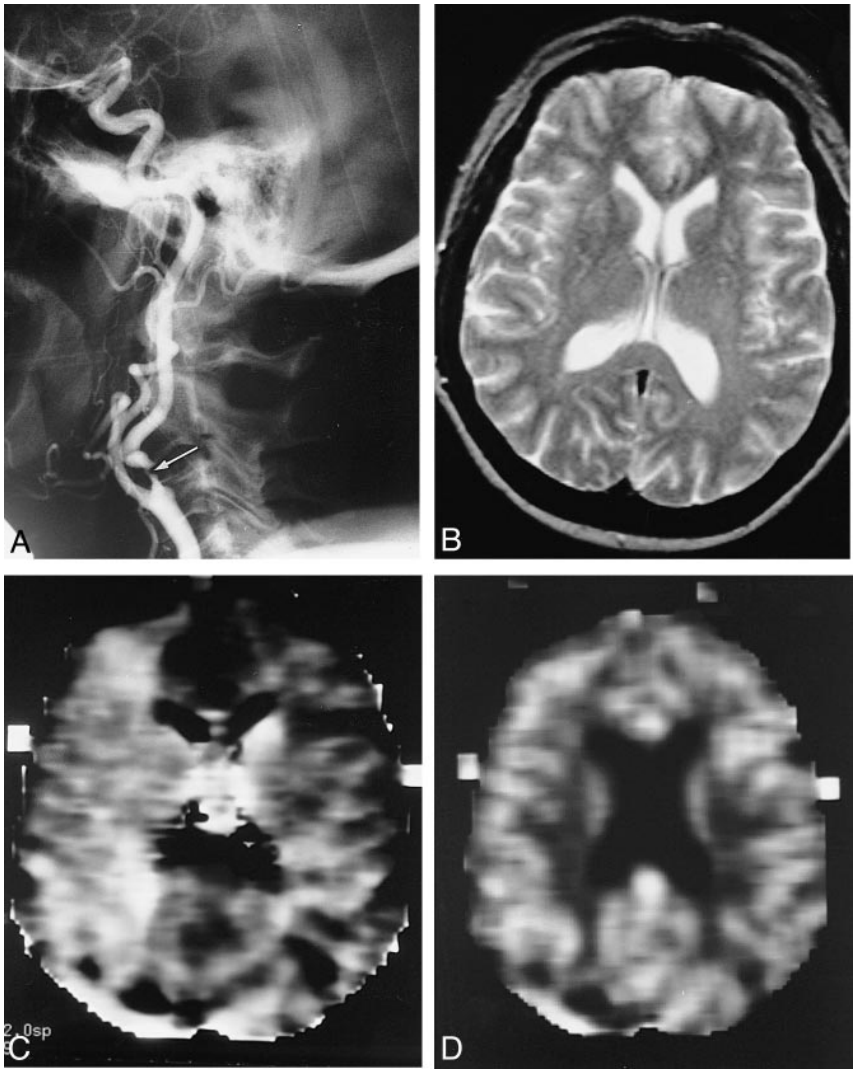

FIG 1. Patient 2: 62-year-old woman with TIAs.

A, Angiogram shows 95% stenosis of the right ICA (*arrow*).

B, Findings on T2-weighted MR image are normal.

C, Corresponding MTT map shows extensive high signal intensity in the right MCA distribution, indicating prolonged MTT on the affected side compared with the contralateral side.

D, Corresponding CBV map shows symmetry in signal intensity, indicating normal CBV.

Qualitative Analysis of EPPI

Qualitative analysis of the rMTT maps and the rCBV maps is summarized in Table 1. Large areas of high signal intensity (prolonged rMTT) were clearly shown on multiple contiguous images in the vascular distribution of affected vessels in all nine patients with unilateral occlusion or stenosis as compared with the contralateral hemisphere (Figs 1–3). Qualitatively, the extent of involvement and increased signal intensity are proportional to the severity of proximal vessel disease in all cases. Two of the nine patients (patients 1 and 3) with less severe stenosis on angiography (Table 1) had a smaller area of involvement and less signal abnormality (less hyperintensity) in the affected vascular territories (Fig 2) than the other patients (Fig 3). In two other patients with bilateral ICA occlusion, almost the entire territory of the ICA had abnormalities, with greater prolonged rMTT (higher signal intensity) than those of the respective posterior cerebral arteries (Fig 4). Four patients had old watershed infarctions with prolonged rMTT (Fig 3).

The findings on the rCBV maps were much less impressive than the findings on the corresponding rMTT maps (Fig 3). Qualitatively, no decrease in the rCBV of the regional hypoperfused tissue (shown by prolonged rMTT) along the 13 vascular distributions was found in any of the 11 patients (normal or increased). On the rMTT maps, the abnormality involved both cortex and white matter, whereas the area of increased rCBV was limited to the cortex or deep gray matter (Fig 3). An increase in regional rCBV on the affected side was visually identified in three patients with unilateral occlusion or severe stenosis of the ICA (Table 1 and Fig 3). The angiograms in these three patients with increased rCBV showed the presence of collateral circulation outside the circle of Willis (via the ophthalmic system in two patients and the meningeal collaterals in one patient). The rCBV maps in the remaining eight patients showed no evidence of rCBV changes on the affected side (Figs 1, 2, and 4). In patients with old watershed infarctions, mildly decreased rCBV was seen in the areas of gliosis (Fig 3B).

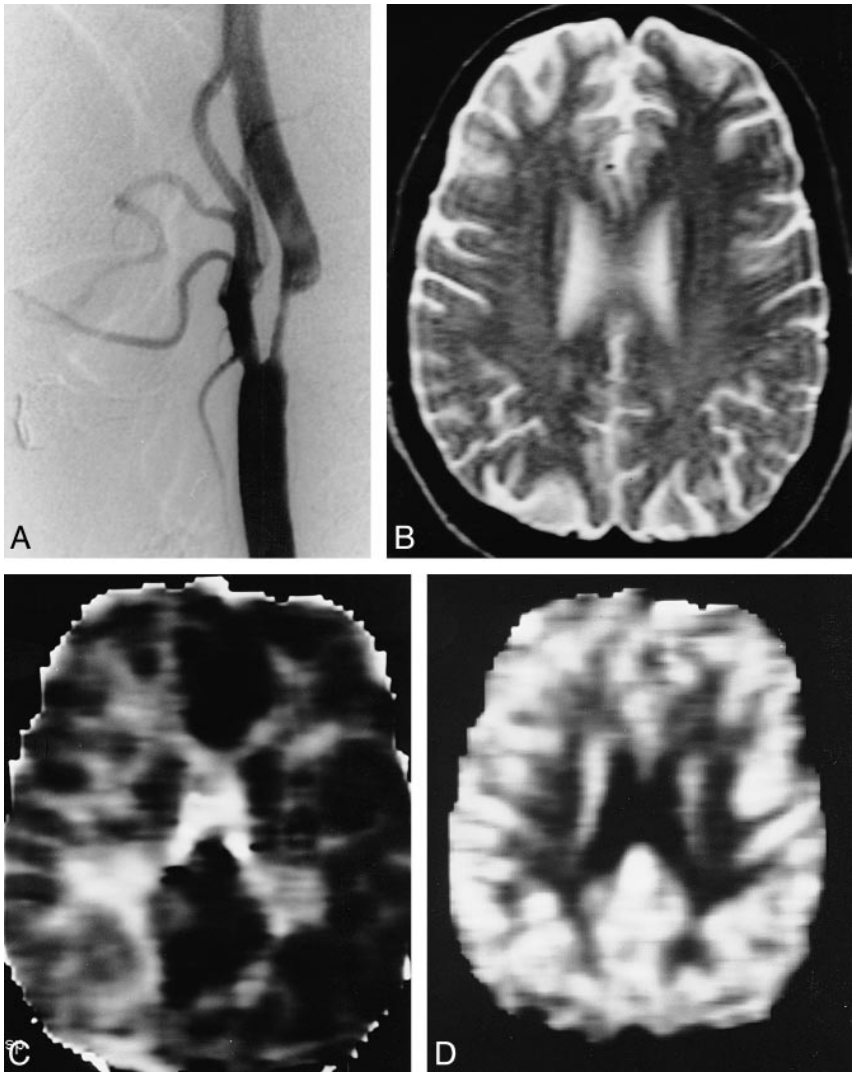

FIG 2. Patient 3: 62-year-old woman with TIAs.

A, Angiogram shows 80% stenosis of the right ICA.

B, Findings on T2-weighted MR image are normal.

C, Corresponding MTT map shows high signal intensity in the right MCA distribution. The extent of high signal is less than that in patient 2 (Fig 1C).

D, Corresponding CBV map shows symmetry in signal intensity.

Quantitative Analysis

The mean rMTT and rCBV values in each case are summarized in Table 2. A significant difference was found in the mean rMTT values along the vascular territories of abnormal vessels ($P < .01$) compared with the contralateral territories. However, no statistical significance ($P = .18$) in the mean rCBV was found, probably because of the small patient population. In retrospect, mild and subtle elevation in the mean rCBV value could be visually appreciated on the rCBV maps in seven of the eight cases previously judged to be ''normal.''

Discussion

Two basic methods are used to measure cerebral hemodynamics in ischemic cerebrovascular disease (2). The first strategy is to measure regional CBF, regional CBV, and regional oxygen fraction in the resting brain using PET (15). The second is to measure both the resting and stimulated brain by acetazolamide, hypercapnia, or a physiological task using single-photon emission CT, xenon CT, or transcranial Doppler imaging (16–19); however, these stimulation methods carry the risk of deteriorating neurologic symptoms. In our study, new techniques of perfusion MR imaging without a vasodilatory stimulus were used to assess the hemodynamic compromise in patients with severe stenosis or occlusion of the carotid artery who had experienced either a recent TIA or minor stroke. In these patients, compensatory changes may have developed that could make evaluation of the underlying hemodynamics challenging, especially at the arteriocapillary (microcirculation) level. On the basis of our limited data, we found that MR perfusion imaging without stimulation can readily and promptly identify the vascular territory responsible for the symptoms and its compensatory changes. Because these patients have neurologic symptoms that are not readily distinguishable from other causes of stroke, identifying the characteristic hemodynamic changes of severe occlusive disease of the carotid artery can be essential to their proper management. With its relative availability and simplicity as compared with PET, EPPI has the potential

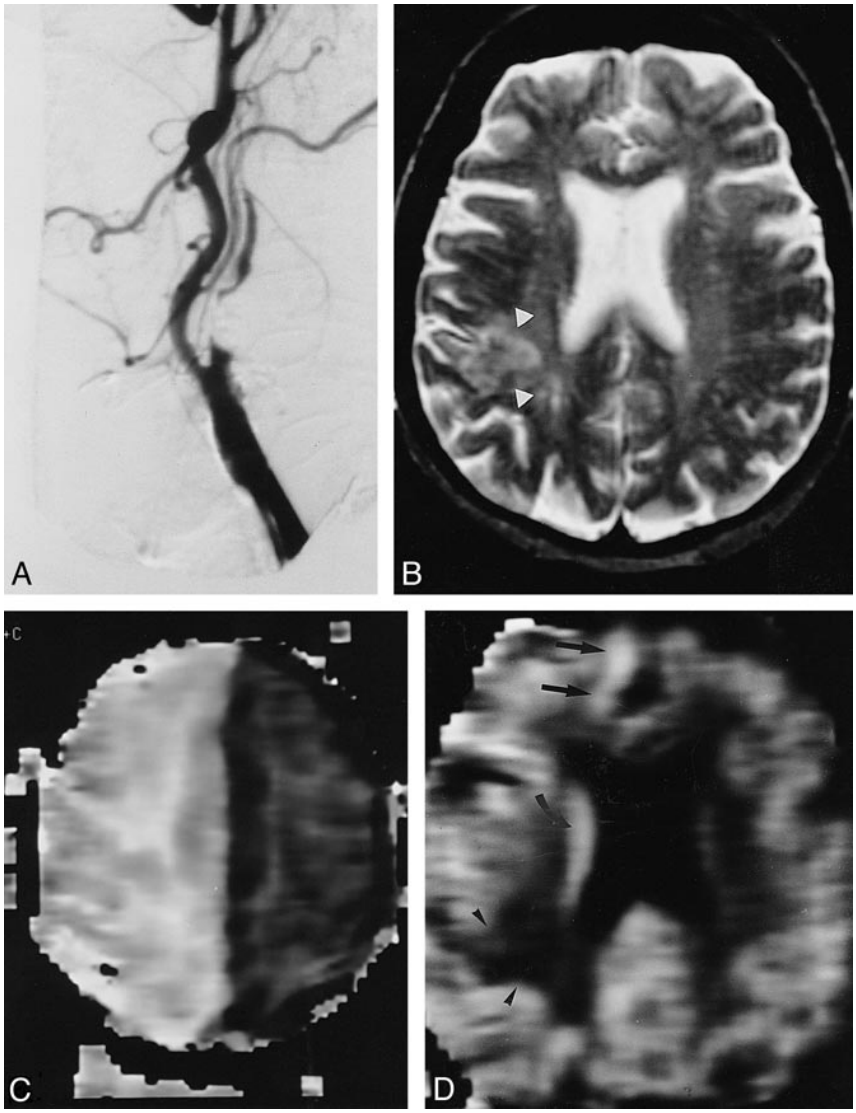

FIG 3. Patient 5: 84-year-old woman with TIAs.

A, Angiogram shows 99% stenosis of the right ICA.

B, T2-weighted MR image shows a right posterior watershed infarction (*arrowheads*).

C, Corresponding MTT map shows extensive high signal intensity in the right MCA and ACA distributions.

D, Corresponding CBV map shows higher signal intensity in the right than in the left ACA distribution (*arrows*), indicating an elevation of CBV in the right ACA distribution. The higher CBV most likely represents brain parenchyma with maximal vasodilatation, while the lower CBV is most likely caused by neuronal loss (old infarction/gliosis) (*arrowheads*).

to improve the diagnosis and management of acute stroke in the chronically hypoperfused brain, even though this technique is only semiquantitative.

Our patients with chronic hypoperfusion frequently experienced transient and/or minor strokes. Although profound restriction of proximal flow was present on the rMTT maps, the rCBV maps showed no abnormalities, indicating that the rMTT maps are best for outlining the tissue with hypoperfusion, including both oligemic (asymptomatic) and ischemic tissue, and rCBV is indicative of the adequacy of compensatory changes, including collateral circulation, to influence ischemic outcome. In our limited patient population, the rMTT maps showed a marked abnormality of the hypoperfused areas along the affected vascular territories. As compared with T2-weighted images, rMTT maps correlate better with the hemodynamic information obtained by angiography: the vascular lesion (stenosis or occlusion) and the macrovascular collateral circulation (ie, circle of Willis and ECA to ICA). This may be explained by the method of deriving rMTT maps by using the characteristics of the arriving bolus of the dynamic study to assess the delay of bolus arrival caused by proximal occlusive disease. This type of information is usually governed by larger-sized vessels (macrovasculature) that can be seen readily at angiography and that influence the result of rMTT. In addition, rMTT maps have been reported to be superior to T2-weighted imaging and cerebral angiography in the evaluation of TIAs and the detection of vascular abnormalities (20). Because of the invasive nature and higher cost of angiograms, rMTT may have the potential to serve as a noninvasive adjunct to screen for possible major arterial occlusive disease before angiography.

The rCBV in patients with severe stenosis or occlusion of the carotid artery was maintained despite severe restriction of the antegrade blood supply revealed by angiography and rMTT maps. The ability to maintain a normal or even increased rCBV in patients with a severe proximal vascular lesion suggests that the hypoperfused brain tissue is likely to

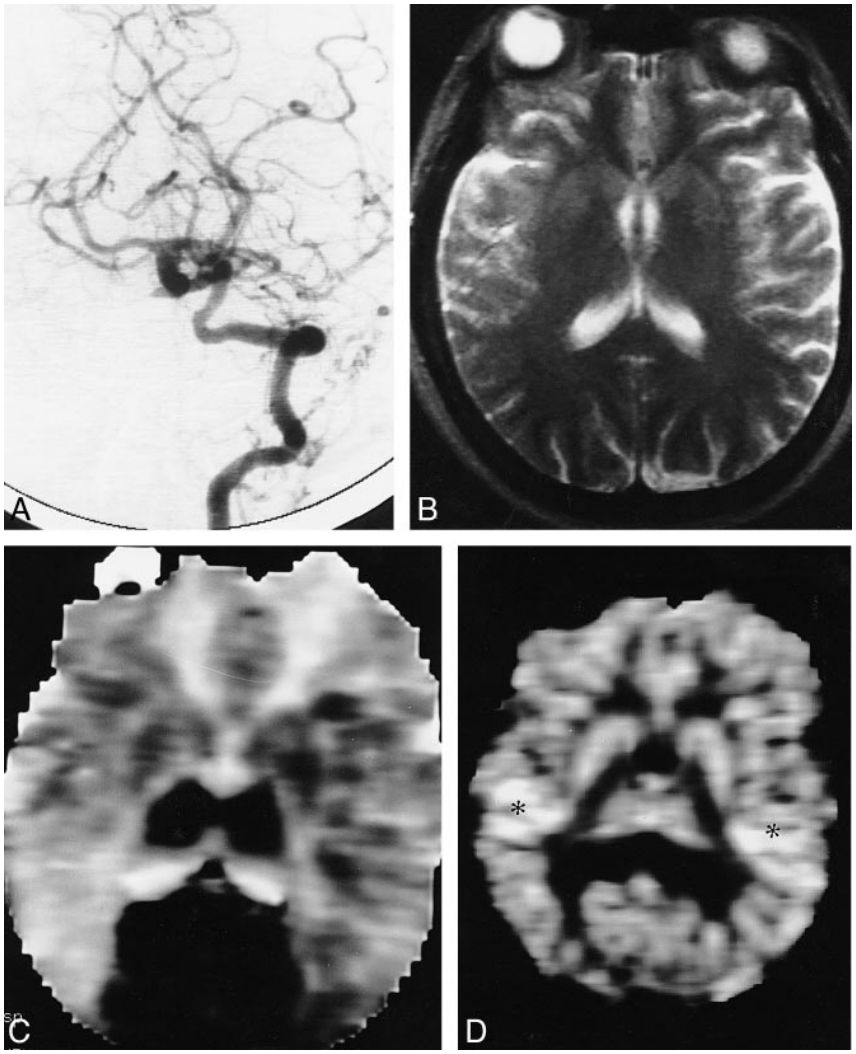

FIG 4. Patient 11: 55-year-old woman with TIAs.

A, Angiogram shows collateral flow to the cerebral hemispheres from the vertebrobasilar distribution through the posterior communicating arteries. Both ICAs were occluded (not shown).

B, T2-weighted MR image shows no abnormalities except for a lacunar infarction on the right.

C, Corresponding MTT map shows extensive areas with prolonged MTT in the distribution of both ICAs. The only normal blood flow is seen alone at both posterior circulations (*dark areas*).

D, Corresponding CBV map reveals no evidence of decreased blood volume. Blood volume is increased in the posterior watershed region bilaterally (*asterisks*).

have adequate collateral circulation to sustain hypoperfusion (oligemia) without persistent neurologic symptoms (CBF $<$ 20 mL/100 g per minute) or major infarction (CBF $<$10 mL/100 g per minute). In our study, the increased rCBV was found predominately in the gray matter, suggesting that the collateral circulation to maintain the rCBV consisted not only of the macrocirculation identified at angiography (eg, circle of Willis and ECA to ICA) with a size greater than 100 μm but also the angiographically ''occult'' pial arteriocapillary bed (microcollateral circulation) in the region of the cortex (white matter is usually supplied by fewer terminal end arteries without collaterals).

It is likely that not only the collateral circulation but also the physiological vascular dilatation results in an overall increase in rCBV. Increased rCBV was only observed in the cortex or basal ganglia, which again suggests that more microvasculature was found in the gray matter than in the white matter, and that vasodilatation is more prominent in this microvasculature. Proximal restriction of blood flow causes an overall reduction in lobar blood flow. Autoregulation mechanism (vasodilatation) compensates for the decrease in perfusion pressure by reducing the arteriocapillary (microcirculation) resistance to recruit and redistribute blood flow, thus increasing tissue perfusion. Those patients with maximal vasodilatation (increased rCBV) are likely to have more hemodynamic stress of hypoperfusion and have a greater risk of incurring a major stroke in the future than those with minimal vasodilatation (normal rCBV).

Fluid-attenuated inversion recovery (FLAIR) has been reported to be a better imaging technique than multiecho T2-weighted imaging in the evaluation of acute stroke. Therefore, FLAIR imaging has been commonly included in the imaging protocol of stroke, as it is currently at our institution. However, FLAIR imaging was not available at the time of our study. The detection rate of abnormalities in our patient group could have been improved had FLAIR sequences been incorporated into our imaging protocol. The ischemic changes detected by multiecho T2-weighted imaging and/or FLAIR include blood-brain barrier breakdown and gliosis, respectively. FLAIR is likely to be a better technique in the detection of subtle changes of ischemia

TABLE 2: Mean values of MTT and CBV in the affected and contralateral sides

	MTT (s)		CBV	
Patient	Affected Side	Contralateral Side	Affected Side	Contralateral Side
1	17.97	17.72	26.03	26.74
2	18.07	17.37	31.22	30.54
3	18.22	17.65	35.90	35.86
4	20.35	19.66	26.02	25.78
5	22.60	18.90	31.08	30.35
6	20.64	19.45	18.91	17.97
7	20.06	18.60	21.58	20.64
8	43.58	39.20	40.81	32.63
9	23.70	21.78	23.33	22.91

Note.—MTT indicates mean transit time; CBV, cerebral blood volume.

(gliosis) that may have been missed by multiecho T2-weighted imaging and might influence our results. The detection rate between these two techniques may not have been dramatically different because multiecho T2-weighted imaging is still quite useful in the detection of gliosis, particularly that involving the basal ganglia and watershed region. Regarding the detection of acute ischemic changes in our patients with severe occlusive carotid artery disease, both techniques may have limited value, because collateral circulation is most likely to have developed in this group of patients and flow-related changes reflected by the perfusion imaging may not be readily detectable by either technique.

The role of T2-weighted imaging in the detection and delineation of chronically hypoperfused tissue and in the evaluation of hemodynamic stress seems to be minimal on the basis of our limited data. In addition, our results are not in complete agreement with those of Yamauchi et al (21), who reported that the presence of ipsilateral confluent high-intensity areas on T2-weighted images indicated a risk of hemodynamic compromise before the development of major neurologic deficits or infarction in the affected hemisphere in patients with ICA occlusive disease. This result was found in only two of the nine patients (patients 6 and 10) with ipsilateral ICA occlusion. Interestingly, small deep white matter infarctions were actually seen more frequently on the contralateral side (three patients) and did not correlate with the degree of severity of rCBV.

The significance and practicality of obtaining absolute measurements by MR perfusion imaging are a matter of controversy. Our data suggest that absolute measurement is an ideal but may not be necessary in the practical sense. It is unrealistic to perform a long and extensive MR examination in the management of acute stroke patients for the purpose of obtaining absolute or near-absolute measurements. For all practical purposes, the imaging time that allows us to generate all the useful and meaningful parameters must be short, preferably within 15 to 30 minutes in patients presenting with ''brain attack'' (including a TIA, which is a retrospective diagnosis). This type of hemodynamic information can further facilitate patient management, including the need for conventional angiography, assessment of severity and risk of major stroke, and choice of treatment (medical vs surgical). Despite significant improvements in hardware, pulse sequences, and methods to improve quantification of MR parameters reflecting the CBF and CBV of ischemic tissue, it is unlikely that MR perfusion imaging can provide absolute measurements of these parameters (22–26). Even with the addition of arterial input functions, which would increase the processing time, absolute measurements still cannot be achieved, because many inherent factors exist that limit this possibility. First, currently available gadolinium-based contrast agents are not the ideal intravascular medium needed for the absolute measurement of CBF. In addition, signal intensity is not linearly proportional to the concentration of these contrast agents. It is still not well understood how tissue relaxivities are affected after the gadolinium contrast agent leaks into the extracellular space, where the environment that the proton may be interacting with is constantly changing and different even along some vascular distributions. Second, many methods are used in the calculation of the different parameters, using various parts of the dynamic contrast enhancement curve (slope, area, time). Third, the dynamic contrast enhancement curve may not be the same at different MR centers, because it can be influenced by different scanners, hardware (gradient strength and raising time), fast imaging techniques (ways of sampling the k-space, EPI, or non-EPI), and pulse sequences (number of preacquisition excitatory pulses, flip angles, gradient echo versus fast spin echo). Just these few factors mentioned can cause variation in the dynamic contrast curve and limit the ability to obtain uniform as well as absolute measurements of CBF and CBV, even with intra-arterial sampling of gadolinium contrast agents, as is frequently done in PET studies.

Whatever techniques are used to generate the dynamic curve and derive the rMTT or rCBV map, it is generally agreed, and suggested by our limited data, that these semiquantitative MR parameters and maps reflect the severity of hypoperfusion or decreased antegrade CBF (rMTT map) as well as the ability to maintain CBV (rCBV map) by developing collateral circulation and by dilatation of the arteriocapillary bed (microcirculation). Moreover, even if an absolute value of CBF could be obtained, the thresholds for infarction and ischemic penumbra have been reported to vary among individuals, making the effort to obtain absolute values somewhat superfluous (27).

Conclusion

MR perfusion imaging can provide a rapid and convenient means to assess the hemodynamic com-

promise involving both macro- and microvasculature in patients with severe stenosis or occlusion of the carotid artery who have experienced either a recent TIA or minor stroke. The MTT map provides the most obvious findings for the detection and delineation of diminished antegrade CBF in hypoperfused tissue and its macrocollateral circulation. The CBV map provides additional information about the underlying compensatory changes regarding tissue reserve and its vascular response to ischemic stress, particularly at the arteriocapillary level. We believe that this type of capability should be readily accessible in the clinical setting and can be valuable in the management of patients with severe occlusive disease of the carotid artery who had experienced either a recent TIA or minor stroke.

Acknowledgment

We gratefully acknowledge Phyllis Bergman for her expert assistance in the preparation of this manuscript.

References

1. Yonas H, Smith HA, Durham SR, Pentheny SL, Johnson DW. **Increased stroke risk predicted by compromised cerebral blood flow reactivity.** *J Neurosurg* 1993;79:483–489
2. Powers WJ. **Cerebral hemodynamics in ischemic cerebrovascular disease.** *Ann Neurol* 1991;29:231–240
3. Yamauchi H, Fukuyama H, Fujimoto N, Nabatame H, Kimura J. **Significance of low perfusion with increased oxygen extraction fraction in a case of internal carotid artery stenosis.** *Stroke* 1992;23:431–432
4. Warach S, Li W, Ronthal M, Edelman RR. **Acute cerebral ischemia: evaluation with dynamic contrast-enhanced MR imaging and MR angiography.** *Radiology* 1992;182:41–47
5. Maeda M, Itoh S, Ide H, et al. **Acute stroke in cats: comparison of dynamic susceptibility-contrast MR imaging with T2- and diffusion-weighted MR imaging.** *Radiology* 1993;189:227–232
6. Hamberg LM, Macfarlane R, Tasdemiroglu E, et al. **Measurement of cerebrovascular changes in cats after transient ischemia using dynamic magnetic resonance imaging.** *Stroke* 1993;24:444–451
7. Reith W, Forsting M, Vogler H, Heiland S, Sartor K. **Early MR detection of experimentally induced cerebral ischemia using magnetic susceptibility contrast agents: comparison between gadopentetate dimeglumine and iron oxide particles.** *AJNR Am J Neuroradiol* 1995;16:53–60
8. de Crespigny AJ, Tsuura M, Moseley ME, Kucharczyk J. **Perfusion and diffusion MR imaging of thromboembolic stroke.** *J Magn Reson Imaging* 1993;3:746–754
9. Kucharcyzk J, Vexler ZS, Roberts TP, et al. **Echo-planar perfusion-sensitive MR imaging of acute cerebral ischemia.** *Radiology* 1993;188:711–717
10. Aronen HJ, Gazit IE, Louis DN, et al. **Cerebral blood volume maps of gliomas: comparison with tumor grade and histologic findings.** *Radiology* 1994;191:41–51
11. Weisskoff RM, Chesler D, Boxerman JL, Rosen BR. **Pitfalls in MR measurement of tissue blood flow with intravascular tracers: which mean transit time?** *Magn Reson Med* 1993;29:553–558
12. Starmer CF, Clark DO. **Computer computations of cardiac output using the gamma function.** *J Appl Physiol* 1970;28:219–220
13. Berninger WH, Axel L, Norman D, Napel S, Redington RW. **Functional imaging of the brain using computed tomography.** *Radiology* 1981;138:711–716
14. Tzika AA, Massoth RJ, Ball WS Jr, Majumdar S, Dunn RS, Kirks DR. **Cerebral perfusion in children: detection with dynamic contrast-enhanced T2*-weighted MR images.** *Radiology* 1993; 187:449–458
15. Levine RL, Sunderland JJ, Lagreze HL, Nickles RJ, Rowe BR, Turski PA. **Cerebral perfusion reserve indexes determined by fluoromethane positron emission scanning.** *Stroke* 1988;19:19–27
16. Kleiser B, Widder B. **Course of carotid artery occlusions with impaired cerebrovascular reactivity.** *Stroke* 1992;23:171–174
17. Gur AY, Bova I, Bornstein NM. **Is impaired cerebral vasomotor reactivity a predictive factor of stroke in asymptomatic patients?** *Stroke* 1996;27:2188–2190
18. Nighoghossian N, Trouillas P, Philippon B, Itti R, Adeleine P. **Cerebral blood flow reserve assessment in symptomatic versus asymptomatic high-grade internal carotid artery stenosis.** *Stroke* 1994;25:1010–1013
19. Knop J, Thie A, Fuchs C, Siepmann G, Zeumer H. **99mTc-HMPAO-SPECT with acetazolamide challenge to detect hemodynamic compromise in occlusive cerebrovascular disease.** *Stroke* 1992;23:1733–1742
20. Crosby DL, Yuh WTC, Magnotta VA, Simonson TM, Zheng J, Ehrhardt JC. **Comparison of echo-planar perfusion imaging with cerebral angiography and T2-weighted MR in the evaluation of transient ischemic attack.** Presented at the annual meeting of the American Society of Neuroradiology, Chicago, April 1995
21. Yamauchi H, Fukuyama H, Yamaguchi S, Miyoshi T, Kimura J, Konishi J. **High-intensity area in the deep white matter indicating hemodynamic compromise in internal carotid artery occlusive disorders.** *Arch Neurol* 1991;48:1067–1071
22. Pedevilla M, Stollberger R, Bammer R, Schmidt F, Wach P, Ebner F. **Improving the diagnostic reliability of dynamic MR-mammography-ROI vs. pixel-by-pixel evaluation.** In: Lemke HU, Vannier MW, Inamura K, eds. *Computer Assisted Radiology and Surgery.* Amsterdam: Elsevier Science;1997:117–122
23. den Boer JA, Hoenderop RKKM, Smink J, et al. Pharmacokinetic analysis of Gd-DTPA enhancement in dynamic three-dimensional MRI of breast lesions. *J Magn Reson Imaging* 1997;7:702–715
24. Tofts PS. **Modeling tracer kinetics in dynamic Gd-DTPA MR imaging.** *J Magn Reson Imaging* 1997;7:91–101
25. Kenney PJ, Sobol WT, Smith JK, Morgan DE. **Computed model of gadolinium enhanced MRI of breast disease.** *Eur J Radiol* 1997;24:109–119
26. Roberts TPL. **Physiologic measurements by contrast-enhanced MR imaging: expectations and limitations.** *J Magn Reson Imaging* 1997;7:82–90
27. Powers WJ, Press GA, Grubb RL Jr, Gado M, Raichle ME. **The effect of hemodynamically significant carotid artery disease on the hemodynamic status of the cerebral circulation.** *Ann Intern Med* 1987;106:27–35